Supporting Information for “Simultaneously Efficient Light Absorption and Charge Separation in $WO_3/BiVO_4$ Core/Shell Nanowire Photoanode for Photoelectrochemical Water Oxidation”

Pratap M. Rao,[‡§†] Lili Cai,[‡†] Chong Liu,[#] In Sun Cho,[†] Chi Hwan Lee,[†] Jeffrey M. Weisse,[†] Peidong Yang[#$] and Xiaolin Zheng[†]*

[†] *Department of Mechanical Engineering, Stanford University, Stanford, CA 94305*

[#] *Department of Chemistry, University of California, Berkeley, CA 94720*

[$] *Materials Sciences Division, Lawrence Berkeley National Laboratory, Berkeley, CA 94720*

*Corresponding author e-mail: xlzheng@stanford.edu

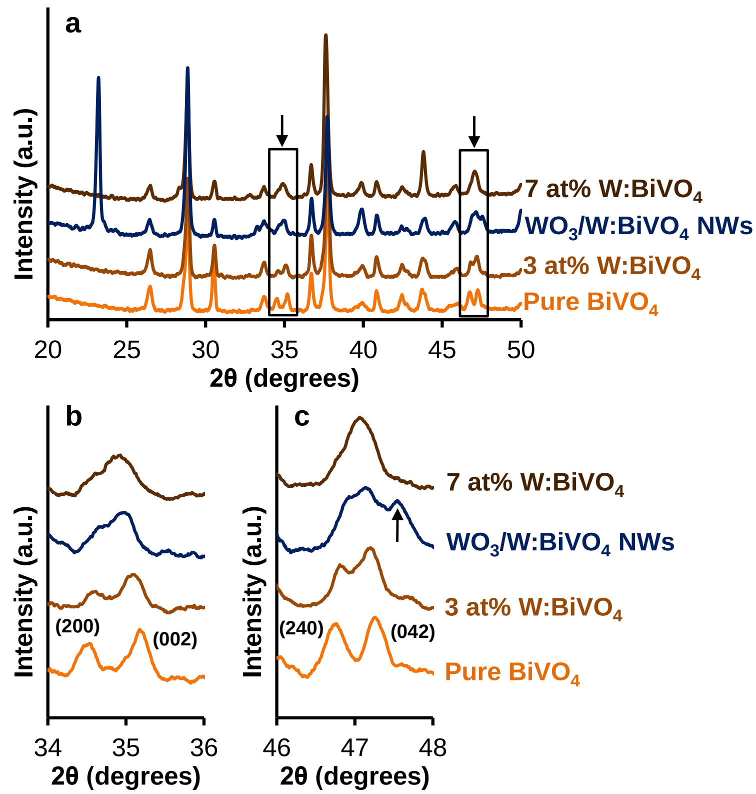

Figure S1. Quantification of the W-doping concentration in the W:$BiVO_4$ shell of WO_3/W:$BiVO_4$ NWs by X-ray diffraction (XRD). As W is doped into $BiVO_4$, the $BiVO_4$ crystal structure becomes distorted.[1] The extent of this distortion is used to estimate the W-doping level in the W:$BiVO_4$ shell of the WO_3/W:$BiVO_4$ NWs by comparison of the XRD pattern of the NWs with those of $BiVO_4$ films prepared with known W-doping levels. (a) The XRD pattern of the WO_3/W:$BiVO_4$ NWs is compared to those of pure, 3% and 7% W-doped $BiVO_4$ films. Consistent with previous reports,[1-4] for the (200) and (002) peaks of undistorted $BiVO_4$ at 2θ = 34.5 and 35.2°, denoted by the left arrow in (a) and enlarged in (b), and the (240) and (024) peaks of undistorted $BiVO_4$ at 2θ = 46.7 and 47.3°, denoted by the right arrow in (a) and enlarged in (c), both converge to form single peaks when the W-doping is 7%, while separate peaks are clearly distinguishable even at 3% doping. Since the peaks in the WO_3/W:$BiVO_4$ NWs have nearly converged, the average W-doping level in the $BiVO_4$ shell is estimated to be about 7%. The peak indicated by an arrow in (c) is due to WO_3.

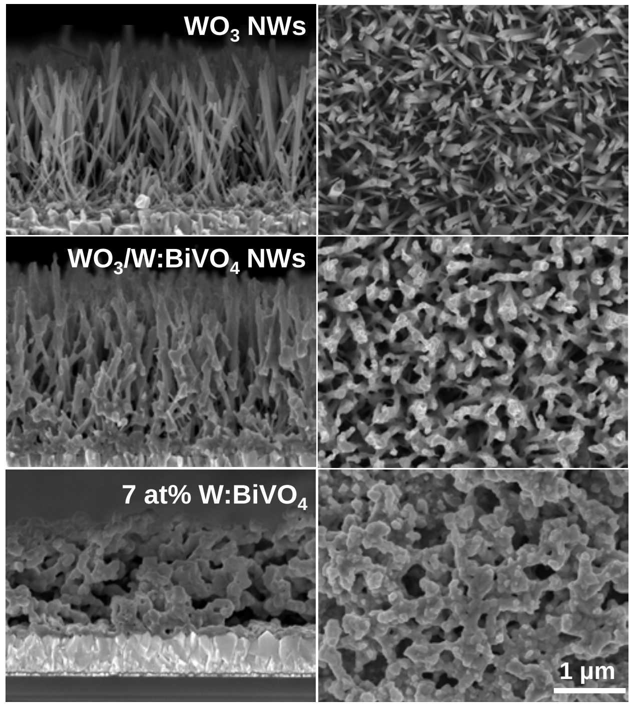

Figure S2. Scanning Electron Microscope (SEM) images of samples synthesized in this work. Left: side view, Right: top view of WO_3 nanowires (NWs), WO_3/W:$BiVO_4$ core/shell NWs and 7 at% W:$BiVO_4$ film (containing the same mass of Bi as coated onto the WO_3 NWs). The scale bar applies to all images in the panel.

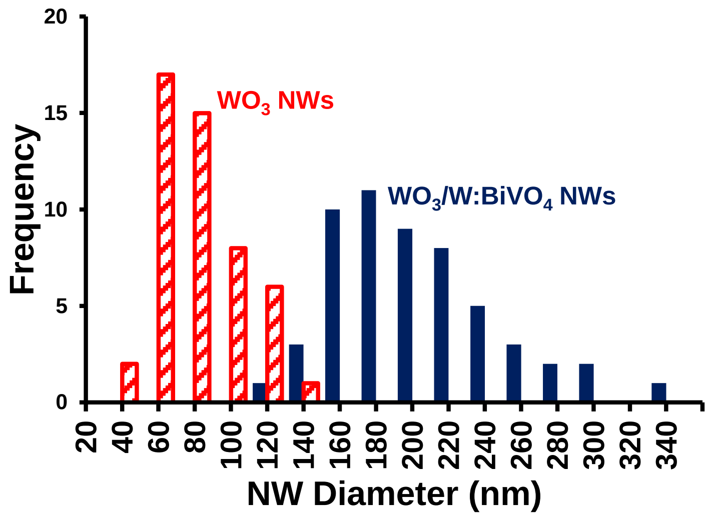

Figure S3. Histogram of diameters of the bare WO_3 NWs and the WO_3/W:$BiVO_4$ core/shell NWs. The bare WO_3 NWs have a 75 nm average diameter and the average W:$BiVO_4$ shell thickness is 60 nm.

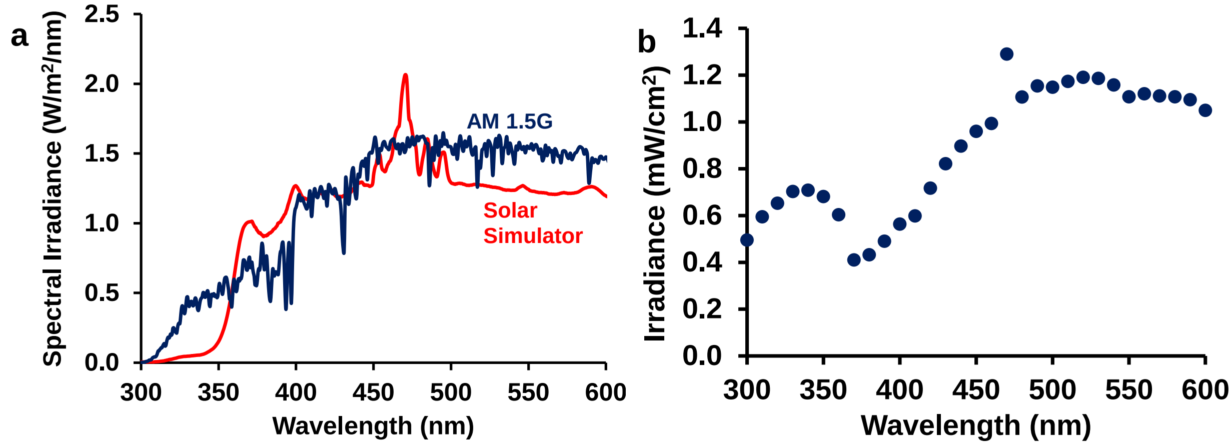

Figure S4. Spectral output of illumination sources used in this work. (a) Spectral irradiance of the class-AAA Solar Simulator (85 mW/cm^2 overall intensity) used to measure current-voltage *(J-V)* curves, measured with a calibrated spectroradiometer, compared to the air mass 1.5 global (AM 1.5G, ASTM-G173-3) standard. For both the simulated illumination and the AM 1.5G standard, the integrated photon current up to a wavelength of 515 nm (the band gap of $BiVO_4$) corresponds to a photocurrent of 7.5 mA/cm^2, thereby indicating that the simulated sunlight is an accurate representation of the standard. (b) Irradiance of Xe lamp with monochromator, used for incident photon-to-current conversion efficiency (IPCE) measurements, measured with a calibrated silicon photodiode.

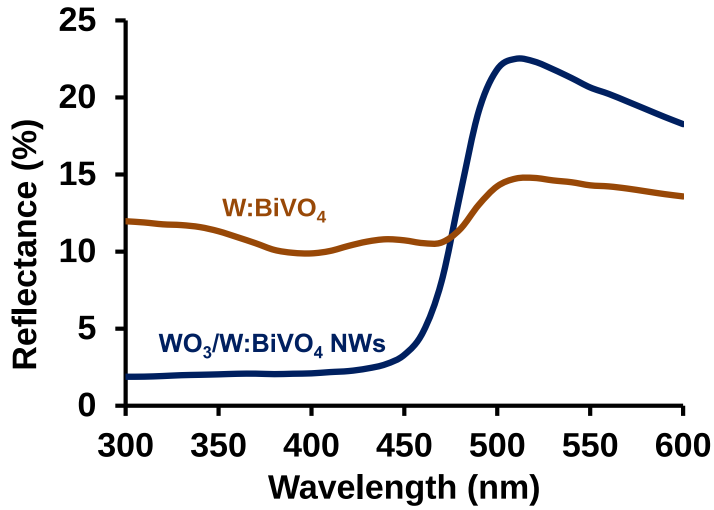

Figure S5. Reflectance of the WO_3/W:$BiVO_4$ core/shell NWs and the 7 at% W:$BiVO_4$ film (containing the same mass of Bi as coated onto the WO_3 NWs).

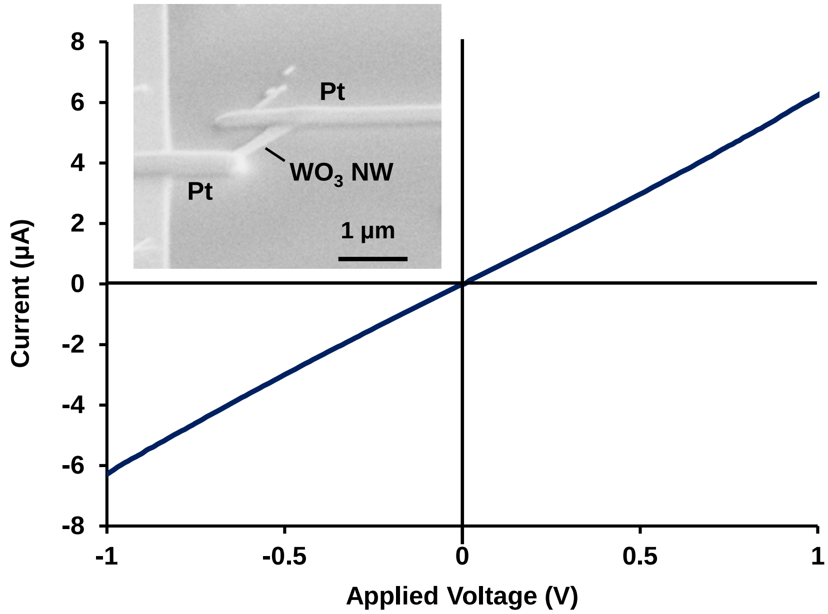

Figure S6. Measurement of conductance of single WO_3 NWs. WO_3 NWs were removed from the growth substrate by sonication in IPA and then drop-casted onto a SiO_2/Si substrate, after which Pt contacts were deposited on both ends of the WO_3 NW using a focused ion beam (FEI Strata DB235). The current–voltage (*I*–*V*) measurements were conducted at room temperature using a semiconductor analyzer (Keithley Model 4200-SCS) with tungsten probes. A measured WO_3 NW is shown in the SEM inset (52° tilt). A conductance of 6×10^{-6} S was calculated based on a current of 6.3 μA at an applied voltage of 1 V, and a conductivity of 5 S/cm was calculated based on the NW diameter of 160 nm and length of 1600 nm (corrected for tilt). Since WO_3 is an n-type material and the measurement was performed in the dark, this is purely a measure of electron conductivity. The measured conductivity closely matches the conductivity of single crystal monoclinic WO_3 NWs with the same [001] growth direction found by others using conductive atomic force microscopy (~1.8 S/cm).[5, 6]

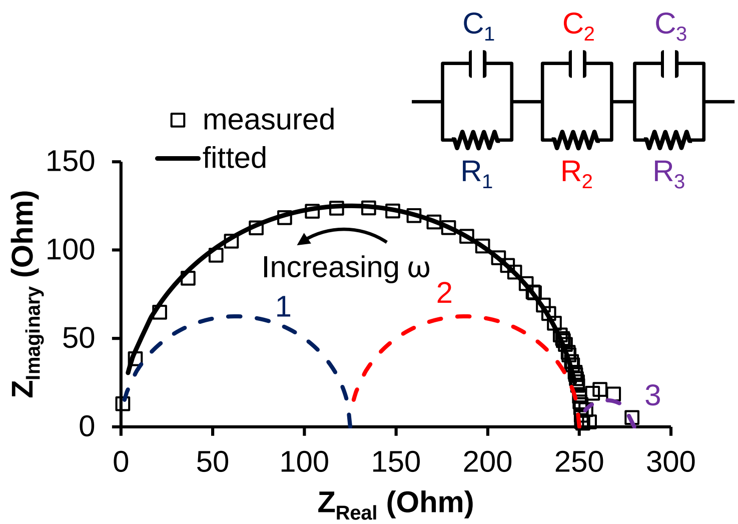

Figure S7. The Nyquist plot from the impedance measurement of a 7% W-doped $BiVO_4$ film, and the equivalent circuit used to fit the measured data. The AC impedance was measured in the dark at room temperature using a 2-probe setup and an impedance analyzer (Agilent Model 4294A) with an applied potential of 500 mV over the frequency range of 40 Hz to 10 MHz. One probe was attached to the exposed surface of a conductive FTO (fluorine-doped tin oxide) glass sheet coated with a 7 at% W:$BiVO_4$ film. The second probe was connected to a piece of adhesive copper tape (Ted Pella) pressed onto the W:$BiVO_4$ film. The Nyquist plot shows a broadened arc which can be decomposed into semicircles by means of the equivalent electrical circuit, which consists of three pairs of parallel-connected capacitors and resistors connected in series. Pair # 1 produces the high-frequency semicircle and is due to the bulk impedance; pair # 2 produces the middle-frequency semicircle and is due to the grain boundary impedance; and Pair # 3 produces the low-frequency semicircle and is due to the film/electrode interface impedance. The bulk conductivity was calculated to be 4×10^{-8} S/cm from the fitted value of R_1 (125 ohm), using the film thickness measured from cross-section SEM images (50 nm), and the area of the copper tape ($1cm^2$). Since W:$BiVO_4$ is an n-type material and the measurement was performed in the dark, this is purely a measure of electron conductivity.

References

1. Park, H. S.; Kweon, K. E.; Ye, H.; Paek, E.; Hwang, G. S.; Bard, A. J. *J. Phys. Chem. C* **2011**, *115*, 17870-17879.
2. Zhong, D. K.; Choi, S.; Gamelin, D. R. *J. Am. Chem. Soc.* **2011**, *133*, 18370-18377.
3. Berglund, S. P.; Rettie, A. J. E.; Hoang, S.; Mullins, C. B. *Phys. Chem. Chem. Phys.* **2012**, *14*, 7065-7075.
4. Pilli, S. K.; Furtak, T. E.; Brown, L. D.; Deutsch, T. G.; Turner, J. A.; Herring, A. M. *Energy Environ. Sci.* **2011**, *4*, 5028-5034.
5. Delamare, R.; Gillet, M.; Gillet, E.; Guaino, P. *Surf. Sci.* **2007**, *601*, 2675-2679.
6. Gillet, M.; Delamare, R.; Gillet, E. *Eur. Phys. J. D* **2005**, *34*, 291-294.